

A Comparative Analysis of GOA (Grasshopper Optimization Algorithm) Adversarial Deep Belief Neural Network for Renal Cell Carcinoma: Kidney Cancer Detection & Classification

M. Sughasiny¹, K.K.Thyagarajan², A. Karthikeyan³, K. Sangeetha⁴, K. Sivakumar⁵

Submitted: 17/10/2023

Revised: 11/12/2023

Accepted: 14/12/2023

Abstract: Renal Cell Carcinoma is a kind of cancer that affects the kidneys. Kidney cancers, also known as RCC, are some of the most devastating illnesses that affect people all over the globe. As a result of the difficulties in recognising kidney cancer at late stages, such as symptoms, the life expectancy is poor; hence, the need of early detection is critical. Kidney cancer detection and therapy are extremely important for early. Existing deep learning approaches based on Deep Belief Neural Networks (DBN) revealed that tuning was an issue of selecting a group of hyper - parameters for the process of learning and contained outliers that influenced the classification outcome. As a result, the goal of this research is to successfully use the Grasshopper Optimization Algorithms (GOA) to perspective of the world unrestricted and restricted multi objective optimization problem. Furthermore, training with the Deep Adversarial Belief Network (DABN) model, that regulated the classifier's behaviour throughout learning, had a substantial effect. The findings indicated that the suggested strategy outperforms current approaches like as, E-CNN method (97%), Fuzzy Particle Swarm Optimization (FPSO) CNN (91.45%), Transferable Texture CNN (98.25%), mask region-based CNN (87.86%) and KNG-CNN (92.4%) in terms of accuracy.

Keywords: Deep Belief Neural Network, Deep Adversarial Network, Grasshopper Optimization Algorithm, Hyper Parameters, Renal Cell Carcinoma- Kidney Cancer, Outliers, restricted and unrestricted Optimization Issues.

1. Introduction

As of 2020, 1.8 million people will have died from kidney cancer, also known as renal carcinoma, and 2.1 million new cancer cases will have been diagnosed. The uncontrolled aberrant development of kidney parenchyma cells causes kidney cancer (Naik and Edla, 2021). Kidney cancer research aids in the development of improved therapies, which improves the quality and length of a patient's life [1]. The study articles show that diagnosis has a deeper and quicker future. Kidney cancer has a greater chance of survival than other cancers, which has prompted more investigation. Because of the large series of thin nephrons that produced an extensive area to exchange gas and continue the process, kidney cancer will develop. Kidney cancer identification at an early stage, according to the World Health

Organization (WHO), leads in a 90 percent chance of survival. As a result, early diagnosis of the condition utilising various examination modalities such as Computed Tomography (CT), X-rays or Magnetic Resonance Imaging (MRI) scans is critical [2-5].

The most common anatomic imaging modalities for detecting Kidney problems are X-ray chest radiography and CT scans (Lyu et al., 2020). Physicians and radiologist examine CT scans to detect disease in the presence of disease visibility, which will immediately expand morphology patterns that define the pathogenicity and track its progression (Singh and Gupta, 2019). As a result, numerous deep learning approaches have been created, including DBNs, which have recently been utilised with promising results for categorising nephron nodule pictures either malignant from benign categories (Nasrullah et al., 2019).

The convolutional layers were used by the DBNs to extract features that exhibited difficulty in the data collected by the final DBN layer. When the middle pooling method was utilised, it include thresholding all of which were retrieved and demonstrated good intricacy (Snoeckx et al., 2018). This roughness review was done out over the picture viewer and also was expensive as matched to pattern with simpler design (Moninuola et al., 2021).

As a result, the suggested technique made advantage of the DBAN layer, which efficiently and effectively examined picture attributes using hyperparameters to develop the training process directly controls the behaviour of either the prediction model and has a substantial influence on the model's performance (Suji et al., 2020). Because of the tuning difficulty of picking a set of hyperparameters for the deep learning model and adding outliers that impact the classification result, the categorization of kidney cancerous tissue into benign and malignant was the most challenging.

To address this problem, the DBAN model was utilised to govern the classifier's behaviour during training, as well as a hyperparameter optimization strategies focused on Grasshopper Optimization to categorise the kidney cancer CT pictures as Malignant or Benign. The findings indicated that the suggested strategy outperforms current approaches like as, E-CNN method

¹Associate Professor, Department of MCA, School of Sciences and Humanities Management, Dhanalakshmi Srinivasan University, Samayapuram, Trichy-612112

Email: sughasinym.som@dsuniversity.ac.in

ORCID: 0000-0003-1880-4595

²Professor & Dean Research, R.M.D Engineering College

Email: kkthyagarajan@yahoo.com

ORCID: 0000-0002-3666-6619

³Professor, Department of ECE,

Sri Sai Institute of Technology & Science,

Rayachoty-516270. Annamaya Dt., Andhrapradesh, India

Email: akarathi_mathi@yahoo.co.in

ORCID: 0000-0003-4279-0808

⁴Associate Professor, Department of CSE,

Panimalar Engineering College, India

Email: sangeethakalyaniraman@gmail.com

ORCID: 0000-0002-7650-6652

⁵Professor, Department of Mechanical Engineering,

P.T. Lee Chengalvaraya Naicker College of Engineering and Technology, Kanchipuram

Email: shivakees@gmail.com

ORCID: 0000-0002-9338-3519

(97%), Fuzzy Particle Swarm Optimization (FPSO) CNN (91.45%), Transferable Texture CNN (98.25%), mask region-based CNN (87.86%) and KNG-CNN (92.4%) in terms of accuracy.

2. Literature Review

Existing lung cancer detection strategies established a deep learning strategy for tumour categorization utilising an effective Kernel-based Non-Gaussian DBN module. For the extraction of input photos, the created model employed the renal Image Database Consortium image collection from LIDC-IDRI. These input pictures were then pre-processed using CLAHE and segmented using the ROI approach. The collected segments were loaded into the KNG-CNN model, which successfully differentiated between malignant and benign growth in lung CT scans. However, in a few situations, the classification results revealed less optimum cancer prediction and kernel approximation.

Ali et al. (2020) created an information layer from which the textural properties of CNN may be used to classify lung nodules using CT images. Using CNN-based Mask R-CNN, which was built for lung area mapping, the generated automated model segmented lung nodules from CT images. Accuracy or other metrics improved using the proposed model. However, the generated system took longer to classify due to the enormous dataset, which necessitated the use of specialist hardware to speed up the training process.

Harsono et al. (2020) built a 13 DR-Net vector quantization training algorithm for lung cancer diagnosis. The current approach used 13DR-Net, a one-stage detector, to solve the issue of lesion classification and categorization. The generated model coupled the artificially high 3D Net backbone's pre-trained natural image weight with the feature pyramid network's feed. The vector quantization learning built successfully categorised lung cancer pictures as malignant or benign tumours. The model, however, was computationally costly, resulting in an economically and environmentally difficult procedure.

Kasinathan et al. (2019) used a Convolution neural contour model to construct an autonomous pulmonary serious illness that achieved segmentation. For the assessment of the findings, the proposed model used the LIDC-IDRI dataset, which generated correct 3D defects in Lung Cancer CT scans. The feature extraction approach was used on 3D pictures, resulting in a deformation procedure that assessed centroid displacement and categorised pulmonary nodules either potentially cancerous tumours. The intensity-based traits, on the other hand, were speed sensitive.

3. Methodology

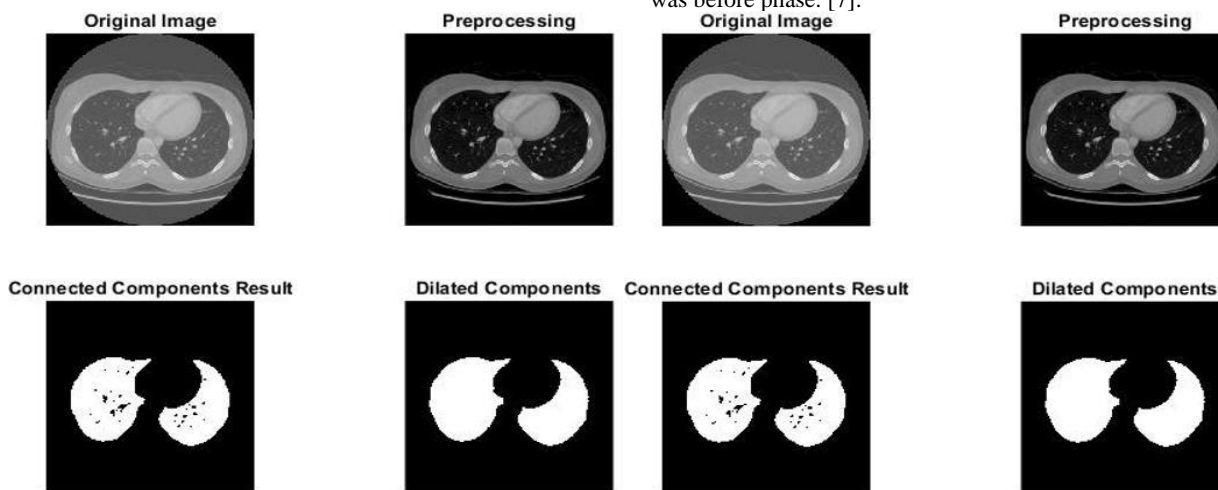


Fig. 2. Sample images from the LIDC-IDRI dataset

Figure 1 depicts the suggested method's block diagram. The following are the stages involved in the suggested hyperparameter optimization.

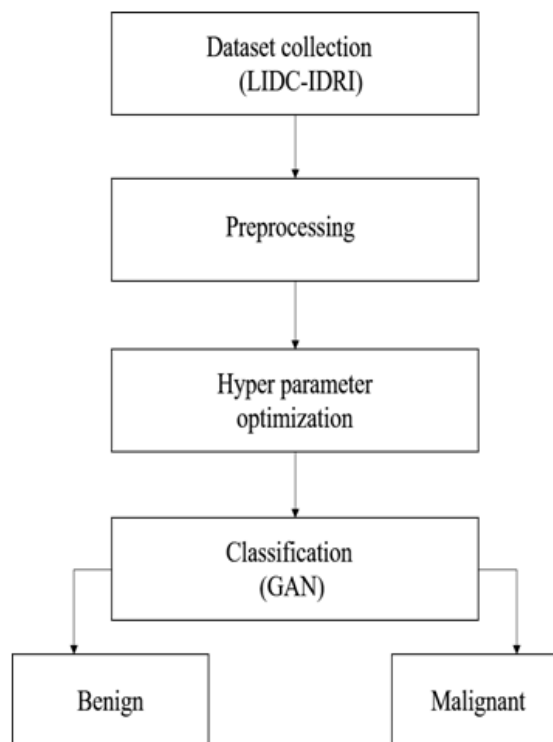
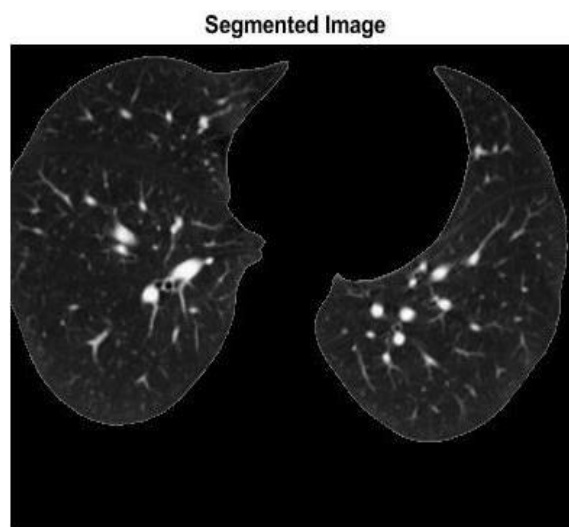
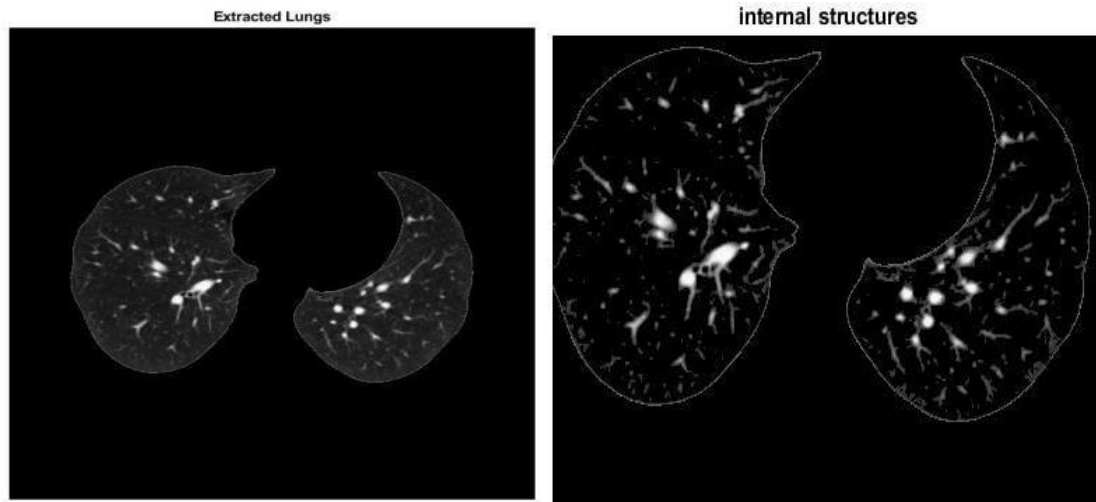


Fig. 1. Block Diagram of the Proposed Method

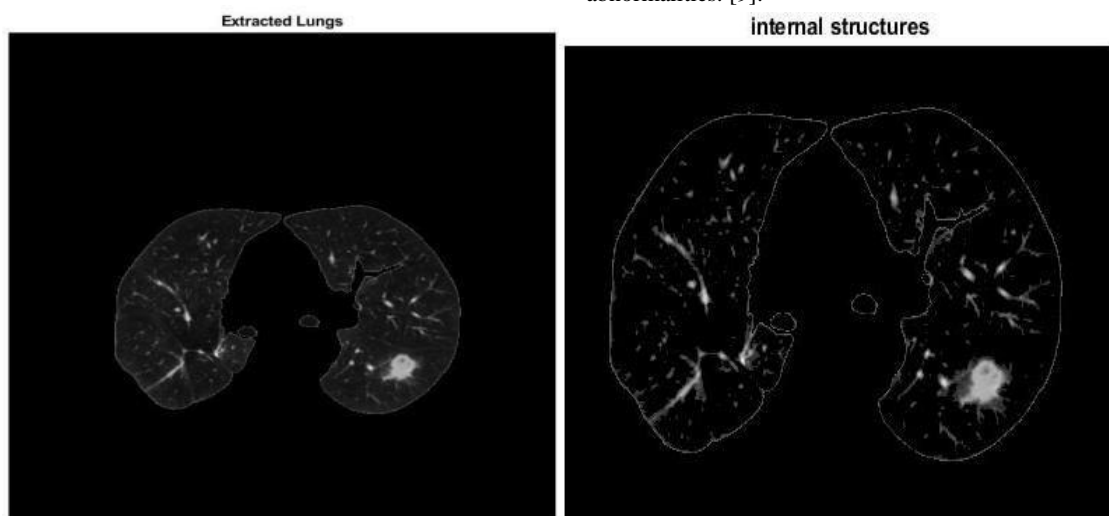
4. Collection of Data

Images of diagnostic abdominal CT scans are coupled including a Xml Schema Communication (XML) annotations for each of individuals. The aggressiveness levels are classified by radiologists into one of five lung nodule classifications. The first three categories will be classified as innocuous, with a class of 0. The malignant classifications that are depicted as class 1 are the other two categories 4 and 5. The suggested technique makes use of the LIDC-IDRI dataset, which contains 2, 44, 527 pictures with digitized radiographs and computational radiographic outputs controlled by a computer. The final conclusion is based on the radiologist's independent examination of their markings, as well as anonymised comments and for three additional radiology. The example photos first from LIDC-IDRI dataset are shown in Figure 2. This pictures and photos will be utilised in the which was before phase. [7].



Images from diagnostic abdominal CT scans are paired with each of the individuals in the XML file. Including a first blindfolded

read phase, it captures the outcomes with a two-phase picture annotation method that mainly skilled thoracic radiologists. Every radiologist examines X rays individually & labels any abnormalities. [9].



Segmented Image

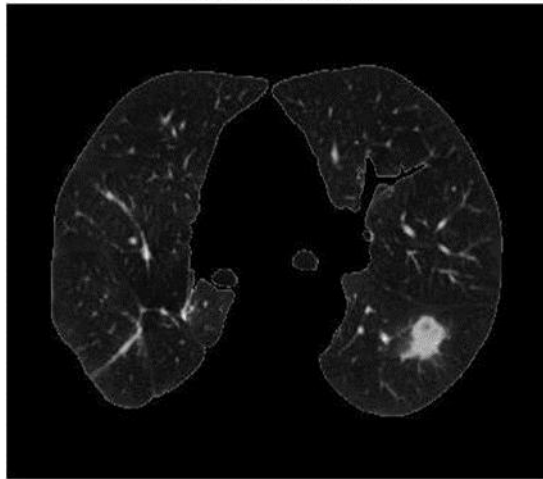


Fig. 3. Segmented images (a) Benign (b) Malignant

4.1 Gaussian Filter for Deionisation

The collected pictures have now been subjected to an image normalisation technique, which converts pixel intensity data to known pixel intensity values. The normalising step is carried out using the Gaussian filter. A Gaussian filtering is applied that blurs the image to lessen the amount of noise in it. The Gaussian filter reduces the contrast level by blurring the edges. The Gaussian filter reduces noises while maintaining crisp edges across all pixels [8].

4.2 Segmentation for Nodule Identification

The relevant sections are segmented, and the remainder part of the image is correctly deleted using the thresholding approach. Thus, pixel separation must be conducted for separating the input pictures into corresponding classes in order to execute this functionality non - linear and non Otsu thresholding. The intensity values are used to create the divided grey levels. Multi-Otsu thresholding is used to compute the threshold values, which will yield the necessary number of classes [10].

Each pixel has an input picture that corresponds to the pixels that are present, and the segmented images and reconstruction of forms from either the given image are illustrated in Fig. 3.

4.3 Hyperparameter Optimization using Grasshopper Optimization Algorithm

Following the removal of noise from the LIDC-IDRI dataset, the suggested hyperparameter optimization procedure is used to tune hyper - parameters depending on melanoma diagnosis. The pixel values of every one of the fully connected layers are modified during the training phase. The governing equations and hyper - parameters that impact the model's behaviour during training are termed even as weighting acquired.

4.4 Grasshopper Optimization Algorithm

The grasshopper optimization approach's major goal is to connect the movements of different grasshoppers to solving the optimization issue, which will reveal both utilisation of motions in the search space. The GOA has a strong inclination to move swiftly toward the present optimal value and chose the factor 1 as a key component in determining the best balance between focused or randomized sweeps by candidate solutions. And used the GOA optimisation with DBAN technique, the optimum parameters values found enable a spectrum for outcomes to prevent the situation of overfitting [12].

4.5 Classification using Deep Belief Adversarial Network (DBAN)

The best computed hyperparameters are now used as inputs again for supervised neural DBAN technique for lung CT image categorization. The DBAN is built on game theory, which is used to connect machine learning models. The DBAN is made up of 2 systems that train simultaneously, with the generator being given

a matrix of sample data as input, which creates data with the same topology as the learning algorithm. The discriminator is fed batches of data including views out from learning of data created output in the network, which distinguishes the view as produced or real. Neural networks are used to implement the two models that were created.

The networks are referred to as a generator in this case, and they will implicitly construct the p model (x) [11]. The discriminator will be given two versions of the generating costs after being trained using the binary classifier. The DBANs will include dual voltage divider and generator networks, which will pull both actual and random data on a continual basis during the training process. The neural network based classifier will be trained using the discriminator. The cognitive development is carried out with the help of the generator, which is unusual in that it does not set explicit objectives for all of the inputs instead merely rewarding the output [12].

5. Results

The outputs of the proposed GOA-DBNN model include sensitivity, accuracy, f-score, and specificity, which are used to show model generalisation.

The simulation results are from an Intel Core i7 processor with a clock speed of 2 GHz and 48 GB of RAM. In this study, 80 percent of the photos are used for training purpose percent are used for testing.

6. Quantitative Analysis

Table 1 demonstrates the results of the suggested GOA-DBAN approach for the LIDC-IDRI dataset with terms of effectiveness, sensitivities, selectivity, MCC, and F-score. For evaluating outcomes and compared them to the suggested GOA and DBAN techniques, innovation and organizational methodologies are applied. For the assessment of the outcomes using the new GOA approach, current methods such as Grey Wolves Optimization (GWO), Ant Lion Optimisation (ALO), and Whale Algorithm Is proposed (WOA) were used. Because of limitations with local searching and a sluggish convergence rate, the GOA had a poor accuracy of 60%. Because the ALO method required additional cycle life till the optimization study, the accuracy values were reduced by up to 90.35 percent. Similarly, the WOA had a sluggish convergence rate, a low accuracy of 95.78, and a tendency to readily slip into the local optimum, resulting in lower accuracy values. The hybrid model of adjusting GOA with DBAN classifiers was employed in this study. The feature subset increased the outcomes by 98.89 percent using the optimization strategy for the grasshopper's mimic behaviour. The assessment of GOA outcomes using known optimization methods. The comparison of DBNN's results with existing categorization methods.

Table 1. Reliability, sensitivities, selectivity, MCC, and F-score are used to evaluate the performance of optimization algorithms.

Optimization approaches	Accuracy (%)	Sensitivity (%)	Specificity (%)	MCC (%)	F1-score (%)
GWO	70.00	71.40	65.45	54.12	64.85
ALO	80.35	87.05	89.56	87.45	89.46
WOA	91.78	89.46	87.75	88.56	91.08
Proposed (GAO)	97.89	87.85	83.32	95.68	96.86

Table 2. Reliability, sensitivities, selectivity, MCC, and score were used to evaluate the classification techniques' performance.

Nets	Accuracy (%)	Sensitivity (%)	Specificity (%)	MCC (%)	F1-score (%)
Alex net	97.54	89.04	92.02	91.21	92.24
Google net	91.45	90.42	91.52	89.54	91.54
VGG16	92.85	89.12	84.85	92.32	93.65
Proposed (DBAN)	96.43	91.86	91.94	96.45	95.85

7. Comparative Analysis

Table 3. Illustrates the results of a comparison of the suggested strategy with current models.

<i>Comparative Table</i>				
Authors	Method	Accuracy (%)	Specificity (%)	Sensitivity (%)
Jena and George (2020)	KNG-CNN	86.30	-	-
Hu <i>et al.</i> (2020)	Mask Region-Based Convolutional Neural Networks	96.68	94.11	97.58
Ali <i>et al.</i> (2020)	Transferable Texture Convolutional Neural Network	98.69	95.37	-
Asuntha and Srinivasan 2020	Fuzzy Particle Swarm Optimization (FPSO)-CNN	95.62	97.32	96.93
Kasinathan <i>et al.</i> (2019)	E-CNN method	96.00	92.00	87.00
Tiwari <i>et al.</i> (2021)	Mask-3 FCM and TWEDLNN a	94.00	96.00	92.00
Nazir <i>et al.</i> (2021)	Laplacian Pyramid (LP) decomposition along with Adaptive Sparse Representation	-	96.00	91.00
Proposed method	GOA-DBAN	97.98	97.67	96.98

Table 2 shows the categorization techniques' precision, sensitivities, particular, MCC, and F-score. Due to data duplication caused by overlapping pixel blocks, the Alex net had a lower error rates of 96.9% and consumed more RAM. In a similar way, a Google Internet classification was used to size the pre-trained model, which produced 92.9 percent higher values than the VGG. The inception model's minimal divergence had a lower accuracy of 90.78 percent. Likewise, the VGG system contains significant weights, however the DBAN framework lowered the amount and gravity of the data, resulting in a gain in energy efficiency of 98.89 percent.

8. Discussion

Jena and George (2020) found that the KNG-CNN classification results had a lower optimality for cancer prediction, as well as a kernel approximation accuracy of 87.3 percent. Masked Area Artificial Neural Networks (Hu *et al.*, 2020) also neglected to consider the labels for each data point, resulting in 97.68 percent greater performance. During big dataset classification, the Directly translatable Multicolor Deep Neural Network (Ali *et al.*, 2020) spent time and hence achieved an accuracy of 96.69 percent.

The created FPSO-CNN (2020) network underperformed during the segmentation phase, showing sluggish divergence during the feature search process 95.62 percent of the time. The intensity-based characteristics of the Enhanced-CNN (E-CNN) approach (Harsona *et al.* 2020) took more computing time and were 97 percent sensitive to speed. Because of the complexity of a troubles, the Mask-3 FCM as well as TWEDLNN achieved an accuracy of 80 per cent, specificity of 97 percent, and sensitivity of 94 percent, and Imran Nazir developed the Laplacian Pyramid

(LP) decomposed automated system only with Flexible Dimension Reduction obtained a responsiveness of 90percent and selectivity of 92 percent.

The suggested GOA-DBAN approach had 96.78 percent efficiency, 97.82 percent sensitivity, and 98.64 percent specificity, demonstrating that using DBAN improved the model's performance. By decreasing the mass & height variables, the model's computation time was lowered.

9. Conclusion

The current study used the Deep Belief Adversarial Network (DBAN) model to train the model, which directly controlled the behaviour of the training and demonstrated a substantial influence utilising the Grasshopper Optimization Algorithm (GOA) on the model's performance. The suggested GOA-DBAN model demonstrated a diminishment and mass function, which reduced the model's calculation and solved the complexity problem. Is because the DBAN model has control over the classifier's behaviour during training, and GOA is very good at solving both unrestricted and constraints of the problem. The suggested approach, the DBAN layer, efficiently and feasibly examined the image attributes. Because of the tuning difficulty of picking a hyperparameter again for training algorithm and integrating aberrations that impact the clustering results, classifying malignant and benign target tissue in the lung is a tough process. The results showed that the proposed method gives better results in terms of accuracy of 97.98% when compared to the existing models The findings indicated that the suggested strategy outperforms current approaches like as, E-CNN method (97%), Fuzzy Particle Swarm Optimization (FPSO) CNN (91.45%), Transferable Texture CNN (98.25%), mask region-based CNN (87.86%) and KNG-CNN (92.4%) in terms of accuracy. In the future, clinicians will be better guided in

evaluating the correctness of each case if the collected nodules are classified by their risk of being benign, aggressive malignancy, or slow-growing.

References

- [1] Armato. (2015). Data From LIDC-IDRI [Data set]. The Cancer Imaging Archive.
- [2] Asuntha, A., & Srinivasan, A. (2020). Deep learning for lung Cancer detection and classification. *Multimedia Tools and Applications*, 79(11), 7731-7762. doi.org/10.1080/0952813X.2015.1020526
- [3] Banerjee, N., Dimitrova, N., Varadan, V., Kamalakaran, S., Janevski, A., & Maity, S. (2017). U.S. Patent No. 9,552,649. Washington, DC: U.S. Patent and Trademark Office. <https://patents.google.com/patent/US9552649B2/en>
- [4] Fedorov, A., Hancock, M., Clunie, D., Brochhausen, M., Bona, J., Kirby, J., ... & Prior, F. (2020). DICOM re - encoding of volumetrically annotated Lung Imaging Database Consortium (LIDC) nodules. *Medical physics*, 47(11), 5953-5965. doi.org/10.1002/mp.14445
- [5] Harsono, I. W., Liawatimena, S., & Cenggoro, T. W. (2020). Lung nodule detection and classification from thorax ct-scan using retinanet with transfer learning. *Journal of King Saud University-Computer and Information Sciences*. doi.org/10.1016/j.jksuci.2020.03.013
- [6] Hadavi, N., Shojaeipour, A., & Nasrudin, M. F. (2020). Classification of normal and abnormal lung ct-scan images using cellular learning automata. *International journal of trends in computer science*, (1). doi.org/10.3844/jcssp.2020.14.24
- [7] Hu, Q., Souza, L. F. D. F., Holanda, G. B., Alves, S. S., Silva, F. H. D. S., Han, T., & Reboucas Filho, P. P. (2020). An effective approach for CT lung segmentation using mask region-based convolutional neural networks. *Artificial intelligence in medicine*, 103, 101792. doi.org/10.1016/j.artmed.2020.101792
- [8] Jena, S. R., & George, S. T. (2020). Morphological feature extraction and KNG - CNN classification of CT images for early lung cancer detection. *International Journal of Imaging Systems and Technology*, 30(4),1324-1336. doi.org/10.1002/ima.22445
- [9] Kasinathan, G., Jayakumar, S., Gandomi, A. H., Ramachandran, M., Fong, S. J., & Patan, R. (2019). Automated 3-D lung tumor detection and classification by an active contour model and CNN classifier. *Expert Systems with Applications*, 134, 112-119. doi.org/10.1016/j.eswa.2019.05.041
- [10] M. J., Van Schil, P. E., van Meerbeeck, J. P., & Parizel, P. M. (2018). Evaluation of the solitary pulmonary nodule: Size matters, but do not ignore the power of morphology. *Insights into imaging*, 9(1), 73-86. doi.org/10.1007/s13244-017-0581-2
- [11] Suji, R. J., Bhadouria, S. S., Dhar, J., & Godfrey, W. W. (2020). Optical flow methods for lung nodule segmentation on LIDC-IDRI images. *Journal of Digital Imaging*, 33(5), 1306-1324. doi.org/10.1007/s10278-020-00346-w
- [12] Tiwari, L., Raja, R., Awasthi, V., Miri, R., Sinha, G. R., Alkinani, M. H., & Polat, K. (2021). Detection of lung nodule and cancer using novel Mask-3 FCM and TWEDLNN algorithms. *Measurement*, 172, 108882. doi.org/10.1016/j.measurement.2020.108882
- [13] Zhang, H., Gu, Y., Qin, Y., Yao, F., & Yang, G. Z. (2020, October). Learning with sure data for nodule-level lung cancer prediction. In *International Conference on Medical Image Computing and Computer- Assisted Intervention* (pp. 570-578). Springer, Cham. doi.org/10.1007/978-3-319-59050-9_20